EUROPEAN FUSION DEVELOPMENT AGREEMENT

EFDA–JET–CP(01)02-20

C.Giroud, K-D.Zastrow, P.Andrew, R.Dux, P.Morgan, M.O'Mullane,
G.Tresset, A.D.Whiteford and JET EFDA Contributors

Neon Transport in JET Plasmas Close to ITB Formation with Monotonic and Reversed q-profiles

Neon Transport in JET Plasmas Close to ITB Formation with Monotonic and Reversed q-profiles

C.Giroud[1], K-D.Zastrow[2], P.Andrew[2], R.Dux[3], P.Morgan[2], M.O'Mullane[4], G.Tresset[1], A.D.Whiteford[4] and JET EFDA Contributors*

[1]Association EURATOM-CEA sur la fusion , CEA Cadarache, F13108, St Paul lez Durance, France.
[2]EURATOM/UKAEA Fusion Association, Culham Science Centre, Abingdon OX14 3DB, U.K.
[3]Max Planck Institut für Plasmaphysik, EURATOM Association, Garching, Germany.
[4]Department of Physics and Applied Physics, University of Strathclyde, Glasgow, United Kingdom
** See the appendix of JET EFDA contributors (prepared by J. Paméla and E.R Solano),*
**See appendix of the paper by J.Pamela "Overview of recent JET results",*
Proceedings of the IAEA conference on Fusion Energy, Sorrento 2000

Preprint of Paper to be submitted for publication in Proceedings of the
EPS Conference,
(Maderia, Portugal 18-22 June 2001)

INTRODUCTION

Recently, optimised shear research at JET has concentrated on two different types of scenario: one with LHCD preheat resulting in a negative magnetic shear and the other with an ohmic preheat leading to a weak positive magnetic shear. The ITB formation and characteristics of these two types of discharge have been studied by systematic variation of input power and torque [1]. In this paper, we study the impact on impurity transport of scenarios for weak positive and negative magnetic shear ITB plasmas.

1. EXPERIMENTAL TECHNIQUE

In this series of discharges, small quantities of neon (less than 0.1%) have been injected during the whole duration of the main heating phase. Ne was injected by edge gas fuelling located on the machine midplane. The valve opening had to be modulated for the gas fuelling system to deliver such a small amount on average. Neon edge lines were not detected by VUV spectroscopy. Neon densities have been measured by charge-exchange recombination spectroscopy (NeX, 5248.5 Å).

Impurity transport coefficients were deduced from a least-squares fit of neon densities modelled by a $1^{1/2}$D transport model code (SANCO) to the measured densities. The neon influx to the plasma is not measured but can be simulated from the pressure drop in the reservoir and knowledge of the fuelling system geometry. The Ne gas is assumed to diffuse with a flux proportional to grad(n^2), n being the density of gas in the fuelling system. Another issue in the determination of transport coefficients is the least-squares fit program. The latter limits the definition of D and V/D profiles to a (changeable) grid of only 4 radial positions connected by straight lines. The least-squares fit program has a constant D and V/D for defined time windows. A smooth evolution of D and V/D from a time window to the next one is not possible at present.

2. DETERMINATION OF IMPURITY TRANSPORT COEFFICIENTS

The transport coefficients are determined for Pulse No's. 51573 and 51598. These discharges correspond to a negative and weak positive magnetic shear ITB plasma, respectively, close to ITB formation at 17MW input power with a dominant normal beam heating. Figures 2, 3, 5 and 6 show the comparison of the experimental data with the SANCO modelled densities.

2.1. JUSTIFICATION FOR THE FIT PULSE NO: 51573:

The delayed appearance of neon in tracks 8, 9 and 10 compared to the rest of the tracks shows a strongly reduced diffusion coefficient in the plasma core. D is determined at ~4.5s and kept fixed for the rest of the discharge. A positive barrier for V/D is required at $\sqrt{Yp_n}$ ~0.45 to reproduce the steep gradient between tracks 6, 7 and 8, and a negative convection is needed for $\sqrt{Yp_n} \leq 0.45$ to explain the time dependence of the density in tracks 8,9 and 10. A close look at the time dependence of Ne density in each track gives information of the ITB time behaviour. The sequence of events, seen in Fig.2, can be explained by an expanding positive (outward convection)V/D region, as shown in Fig.3.

2.2 JUSTIFICATION FOR THE FIT PULSE NO: 51598:

No delay in the appearance of Ne between tracks is observed. The diffusion is therefore kept constant in space, determined at ~ 44.2s and kept fixed in time. Here again, a positive barrier for V/D is required at $\sqrt{\Psi}p_n \sim 0.4$ to reproduce the steep gradient between tracks 6, 7 and 8, but for this pulse a positive convection is required at $\sqrt{\Psi}p_n \leq 0.4$ to reproduce the density time dependence in tracks 8, 9 and 10. Here again, an expanding V/D positive (outward convection) region can explain the density time evolution in each track.

CONCLUSION

We show clear evidence of the dependence on impurity transport of the chosen magnetic shear scenario. Neon accumulates in reversed magnetic shear ITB plasmas, due to inward convection, but not in weak positive shear ITB plasmas, where convection is outwards. Similar conclusions were drawn from the study of the equivalent discharges at 15 MW input power (Pulse No: 51594, Pulse No: 51595). This result is in agreement with the impurity behaviour in high performance discharges [3]. The implications of this work are two-fold. Firstly, there is little hope in controlling the impurity content in negative magnetic shear ITB plasmas. Secondly, there will be no impurity accumulation in weak positive magnetic shear ITB plasmas if the outward convection can be maintained on a longer time scale.

REFERENCES

[1]. C.Challis, et al., at this conference.
[2]. G.Tresset, et al, at this conference.
[3]. R.Dux, et al, at this conference.

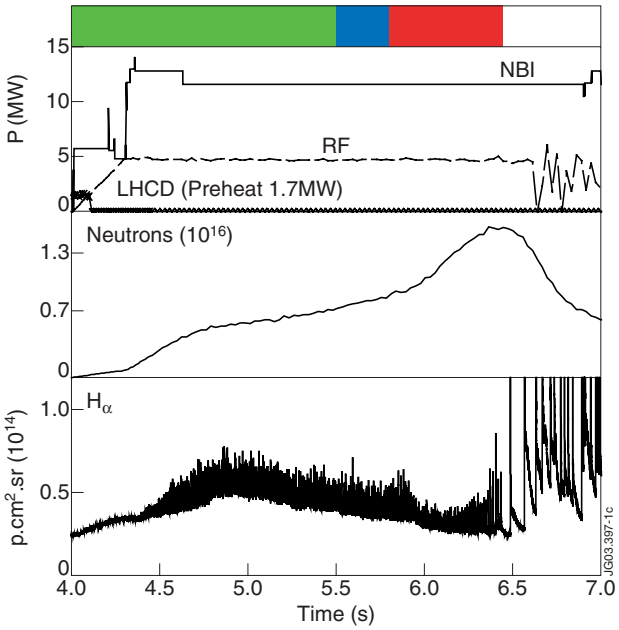

Figure 1: Time evolution of the Pulse No: 51573.

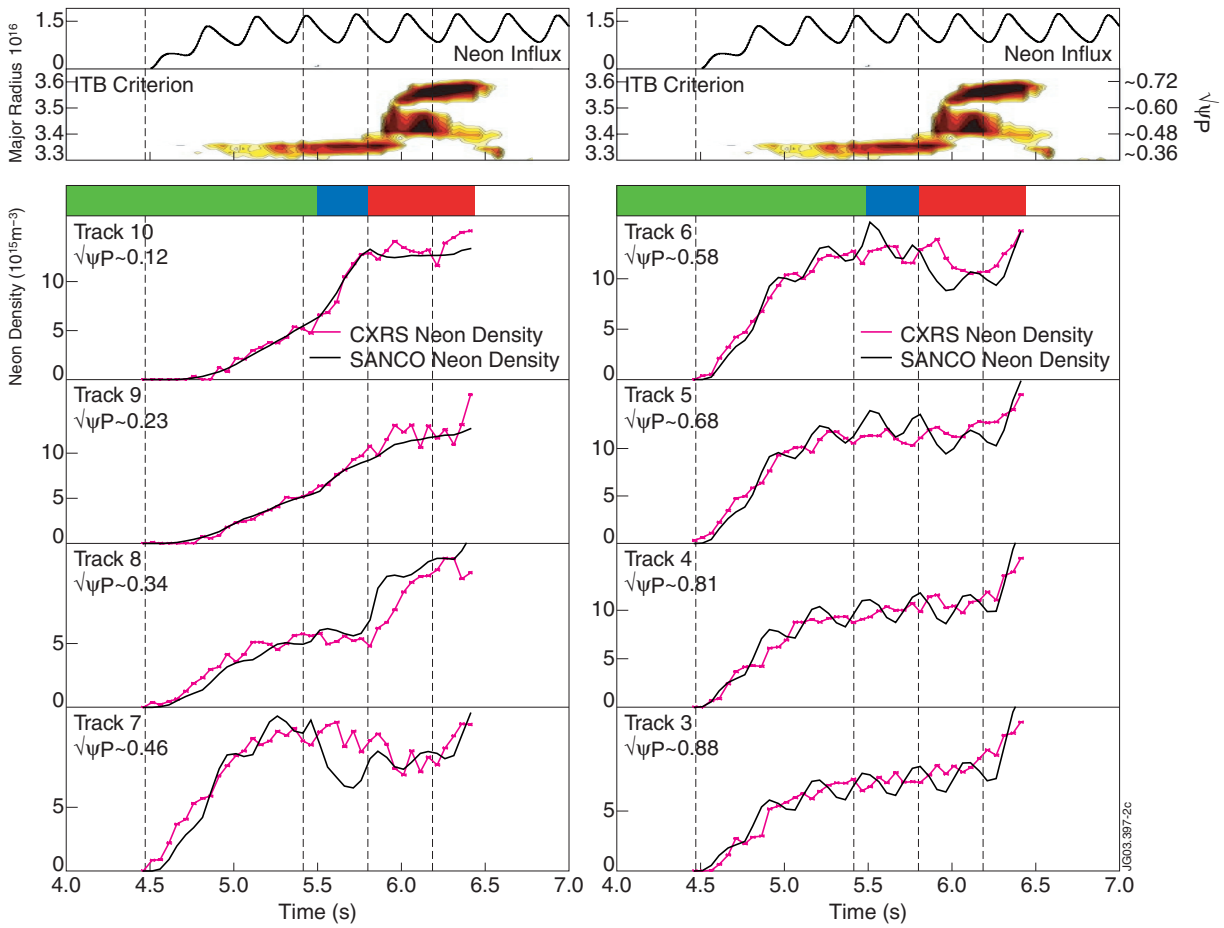

Figure 2: (from top to bottom) Simulated neon gas influx to the plasma used in SANCO. ITB Criterion: contour plots of ρ^*_T, [2], showing the strength and position of the barrier: the darker the colour, the higher ρ^*_T, the stronger the ITB. Defined time slices for χ^2 fit: the coloured rectangles indicate the time slices used in the χ^2 fit. Time evolution of NeX density measured by CXRS in the different CCD tracks (in pink) compared to SANCO modelled density (in black). Ψp is the normalised poloidal flux.

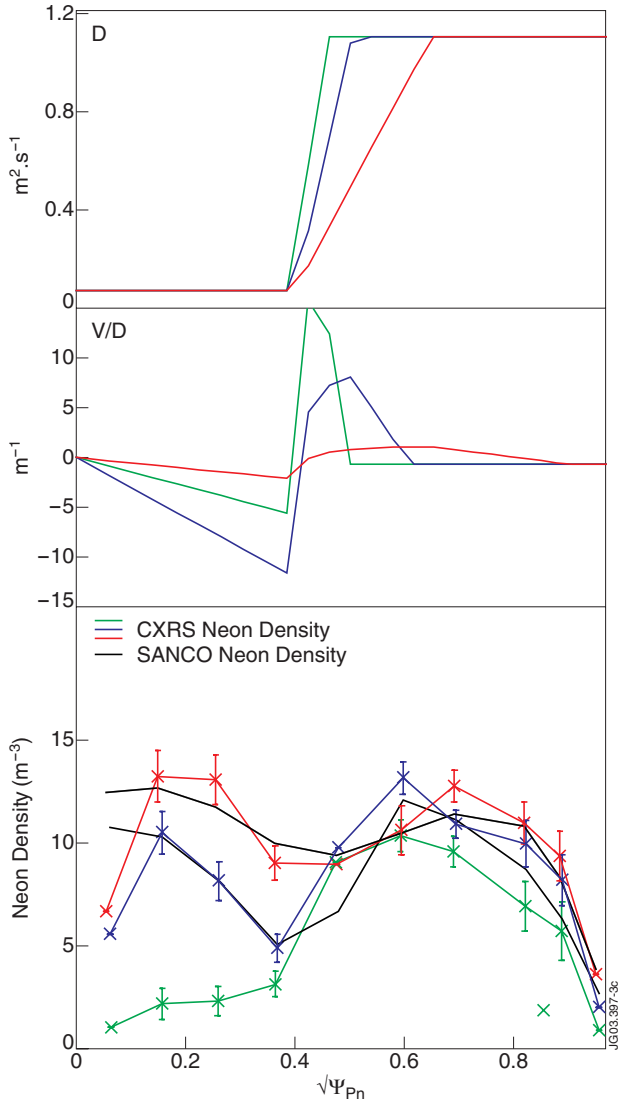

Figure 3: (from top to bottom) Profiles of the diffusion coefficient (D) and V/D against $\sqrt{\Psi p_n}$ used in the χ^2 fit, V being the convection coefficient and Ψp_n the normalised poloidal flux. Typical measured and modelled NeX densities against $\sqrt{\Psi p_n}$ during the different time slices. Tracks plotted without error bars were not considered in the χ^2 fit.

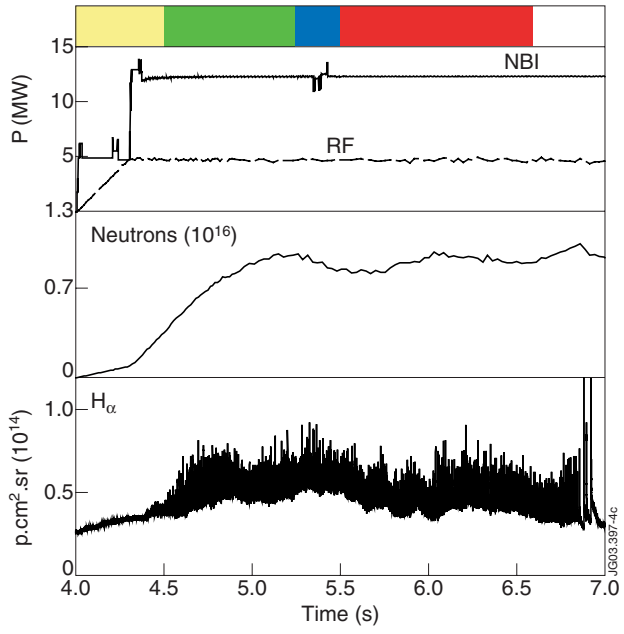

Figure 4: Time evolution of the Pulse No: 51598.

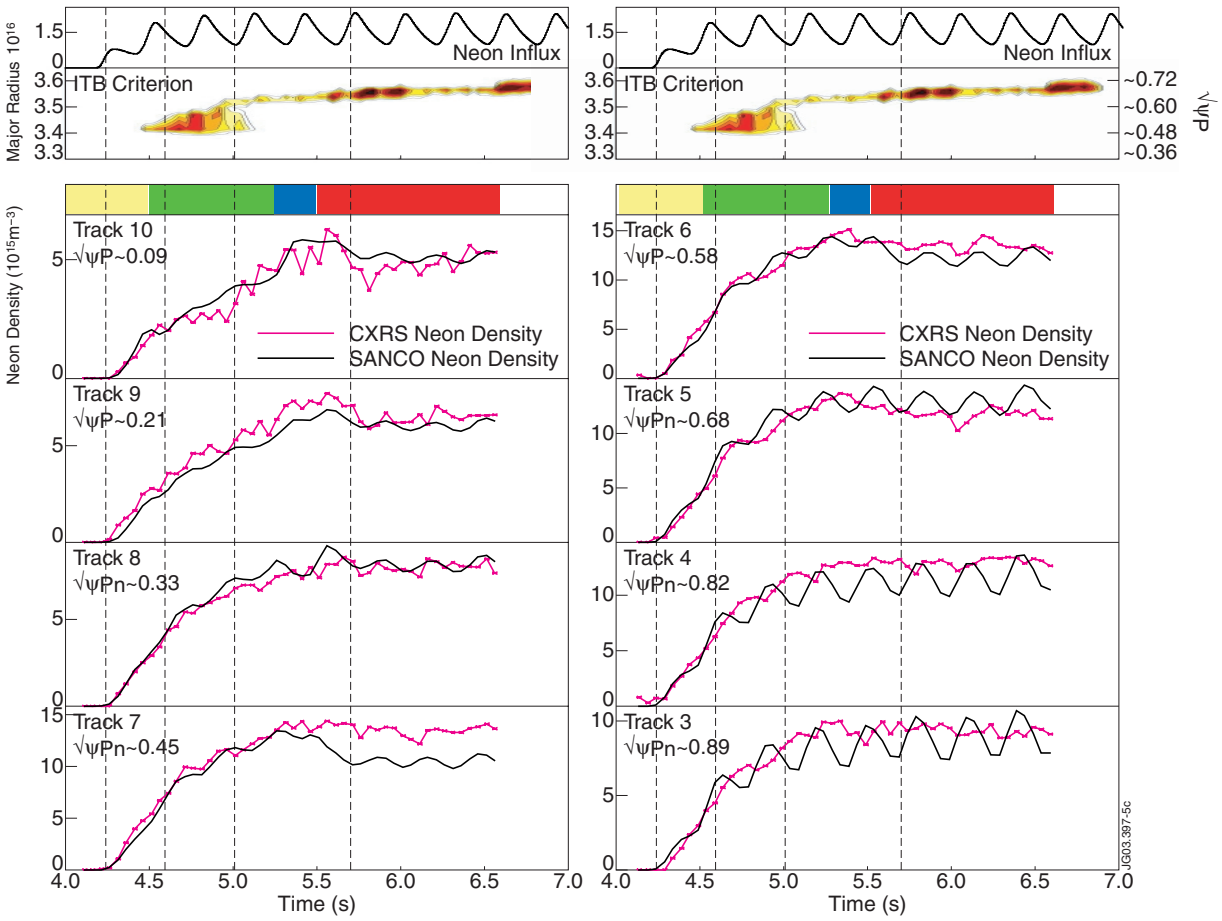

Figure 5: As in figure 2 for Pulse No: 51598.

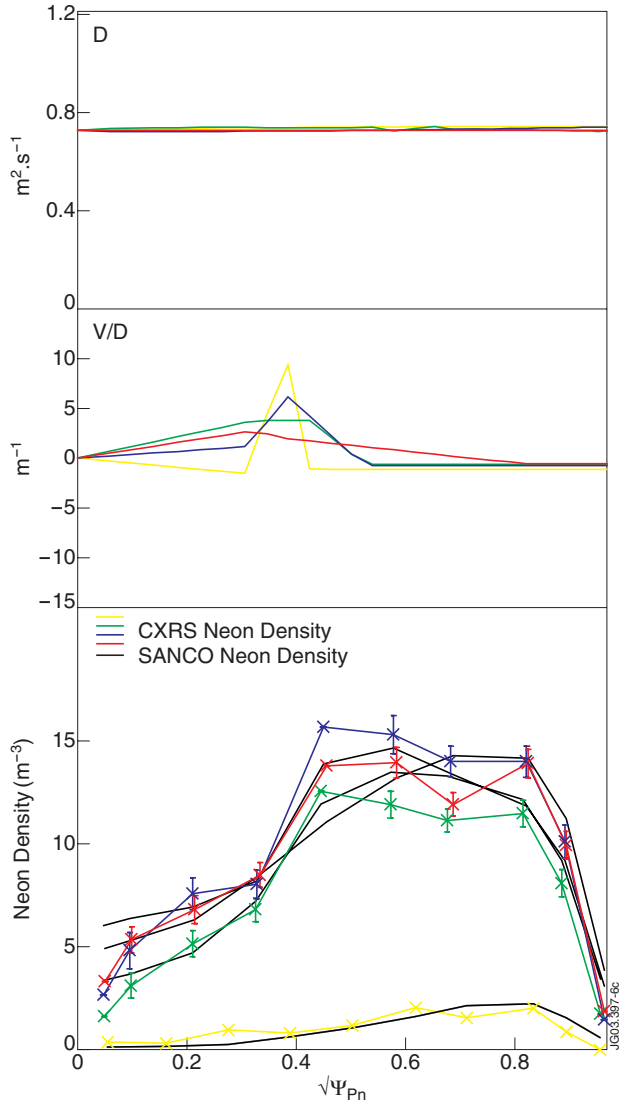

Figure 6: As in figure 3 for Pulse No: 51598.